2464-1

Earthquake Tectonics and Hazards on the Continents

17 - 28 June 2013

The nature of the hazard: Introduction to earthquakes, their sizes, intensities, and distribution in space and time (continents vs oceans and plate tectonics)

P. England
*University of Oxford
UK*

INTERNATIONAL CENTRE FOR THEORETICAL PHYSICS

Earthquake Tectonics and Hazards On The Continents

June 2013

Background Material

This handbook is intended to give you some background to the subjects covered in the first week of the Summer School. If you already know a lot about earthquakes, you may not need to read this handbook. If you know little about earthquakes, do not be alarmed if the material is unfamiliar to you: by the end of the Summer School, you will be in a position to use this knowledge.

Why and how are the Tectonics of Continents and Oceans Different?

Synopsis

The simple concepts of Plate Tectonics, which were so successful in describing the deformation of the ocean basins, are not easily applicable in continental tectonics, where the deformation is usually much more diffuse than in the oceans, and not restricted to narrow plate boundaries. A different framework is needed for viewing continental deformation. The continental lithosphere consists of a thin (10–20 km) 'brittle' layer above a much thicker (80–100 km) layer that probably deforms by distributed creep. The scale on which major topographic features, such as mountain belts, plateaus, and basins, occur suggests that at long wavelengths the deformation is dominated by the behaviour of the creeping lower lithosphere and is best described by a continuous velocity field. An important problem is then to obtain this velocity field and understand its relation to the motions of the rigid plates that bound the deforming region.

There are three fundamental scales in the deformation of the lithosphere: the thickness of the seismogenic layer; the thickness of the crust and the thickness of the continental lithosphere itself. Continental and oceanic lithosphere differ at all three of these scales, and in fashions that influence crucially their response to deviatoric stress. The seismogenic layer is generally 10–20 km thick in the continents, and the crust is generally 20–70 km thick. Thus there is a substantial fraction of the continental crust which deforms aseismically, and presumably by the mechanisms of crystal plasticity and dislocation creep. In contrast, the oceanic crust is generally less than 10 km thick, but earthquakes in the oceanic lithosphere occur to depths of several tens of kilometres. The differences in the mechanical behaviour of these two lithospheric types is explained by the differences in their thermal structure, as well as by differences in the strengths of the principal minerals of the respective columns. It seems likely, from laboratory determinations of the strengths of rocks and minerals, and from determinations of deviatoric stress from major fault zones, that the upper limit to the strength of the continental lithosphere is ∼100 Mpa (about 1 kbar), whereas the oceanic lithosphere is capable of supporting deviatoric stresses considerably higher than this value – and to greater depths. The other major difference between continental and oceanic lithosphere is the greater thickness, and lower density of the continental crust. Contrasts in crustal thickness within deforming continental lithosphere introduce deviatoric stresses which are analogous to the 'Ridge Push' driving force of Plate Tectonics, but can greatly exceed this force in magnitude. Oceanic lithosphere, with its greater strength, can support these driving forces without deforming permanently, but continental lithosphere cannot. In consequence, forces associated with crustal thickness contrasts play an important part in continental deformation, and account for much of the richness of tectonic style exhibited in zones of active deformation.

Observations of Deformation Plate tectonics requires measurement of velocity and strain around plate margins. Observations of earthquakes and topography show that continental deformation is pervasive through large regions of the continents. These observations pose the question: What are the rules that govern continental deformation?

The lithosphere The lithosphere has petrological, seismological, mechanical and thermal definitions. The fundamental definition is thermal, and thicknesses defined by other means may be referred to thermal definition, and variations in these thicknesses are largely related to thermal variations.

1. The lithosphere forms the upper boundary to convection in the mantle. Mantle convection is very vigorous (Rayleigh Number 10^7 or more), so that most temperature variations occur across thin boundary layers in the fluid. The dominant mechanism of heat transfer in the boundary layers is thermal conduction. The top boundary layer is the thermal lithosphere, and temperature drops from $\sim$1300°C at its base to $\sim$0°C at its top.

2. Because of the very strong dependence of the strength of rocks on temperature, the lithosphere varies in its behaviour from a weak fluid at its base to a strong ('rigid' in the case of oceanic lithosphere) elastic solid near its top. The thermal definition of the lithosphere thus includes layers of greatly differing mechanical properties.

3. Two contrasting layers are often identified within the thermal lithosphere: the Mechanical Boundary Layer, which is the portion of the lithosphere that is much stronger than the asthenosphere and which does not participate in mantle convection, except where it is subducted, and the *fluid* Thermal Boundary Layer, which is not appreciably different in properties from the underlying upper mantle, but happens to be transferring heat by conduction.

Driving Forces Driving forces on the lithosphere are probably 10^{12}–10^{13} N m^{-1} (10 MPa–100 MPa averaged over a 100 km of lithosphere). These arise either from the driving forces for plate motion, or from crustal thickness contrasts mentioned above.

Deformation Mechanisms Most prominent mechanism of deformation in upper crust is faulting. Byerlee's law commonly assumed to hold. In oceanic interiors, depth of seismicity is consistent with this assumption and zero, or hydrostatic, pore pressure. Observations on major active fault zones in continental interiors, and at plate boundaries, suggest that, if Byerlee's law does hold in these zones, the pore pressure is very close to lithostatic. Continental faults appear, therefore, to be weak. Faulting confined to upper crust; weaker deformation mechanisms in lower crust. Upper mantle deforms seismically in a few places, but contribution of this mechanism to total strength of lithopshere is likely to be small. Estimates of shear stresses in lower crust and upper mantle of order 100 MPa or less.

Continental Deformation

Plate Tectonics?

The central hypothesis of plate tectonics is that the surface motions of the earth can be described by the rigid-body motions of a small number of plates. This hypotheses is expressed in a simple vector relationship:

$$\mathbf{v} = \omega \times \mathbf{r} \qquad (1)$$

where $\mathbf{v}$ is the relative velocity of one plate with respect to another at a point on the earth's surface defined by a radius vector, $\mathbf{r}$, and ω is the relative angular velocity of the two plates.

This hypothesis gained rapid acceptance because it was simple to test, by making measurements of relative motions at widely-spaced points around the edges of plates, without the need for measuring velocities in the plate's interior [*De Mets et al.*, 1990; *Isacks et al.*, 1968; *McKenzie and Parker*, 1967; *Morgan*, 1968]. Unfortunately, in all important aspects, when we try to apply the idea of plate tectonics to the continents we find that it is wrong. The evidence for that statement can be seen on opening any atlas. Certainly the narrow bands of earthquakes at the oceanic ridges, and near subduction zones, attest to the narrowness of the zones where oceanic plates interact, but over large parts of the continents, there are broad zones of shallow earthquakes (Figure 1).

The deformation of continental regions is not confined to narrow bands, but is spread over regions hundreds to thousands of kilometres (see Figures 2 to 6). For example, the region of continental deformation in Asia is larger than the Cocos plate [e.g. *Molnar and Tapponnier*, 1975; *Tapponnier and Molnar*, 1976].
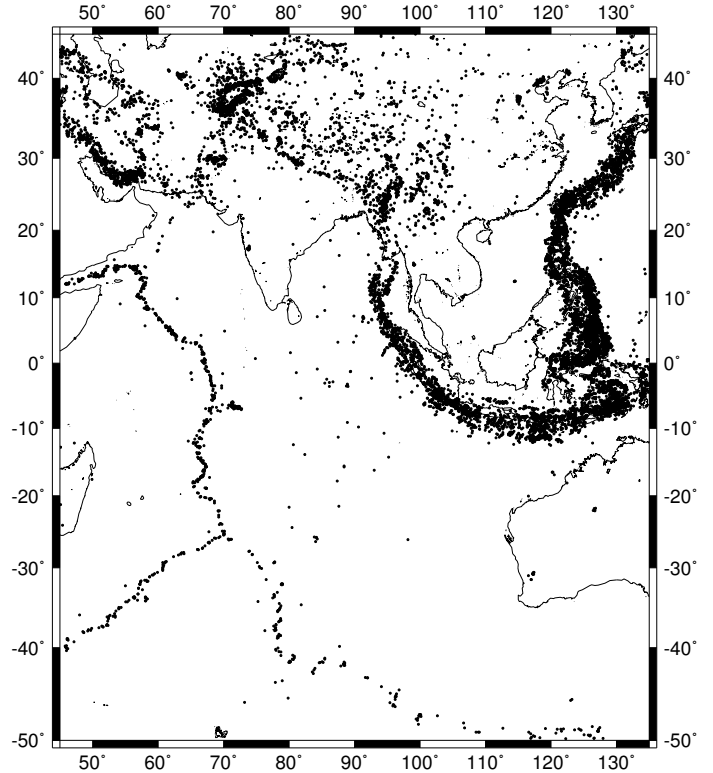
Figure 1: The epicentres of earthquakes occurring in the region of the Indian Ocean between 1964 and 1990. Note the narrowness of the bands of seismicity along the ridges and trenches, in comparison with the distribution of earhtquakes in Asia, where the convergence of India with Eurasia is accommodated within the continental lithosphere of Asia. You can also see part of a smaller zone of continental deformation in Iran (about the size of western Europe). Note that the apparently broad zones of earhquakes along the island arcs are, in fact, the projections onto the surface of narrow, but dipping, bands of hypocentres.
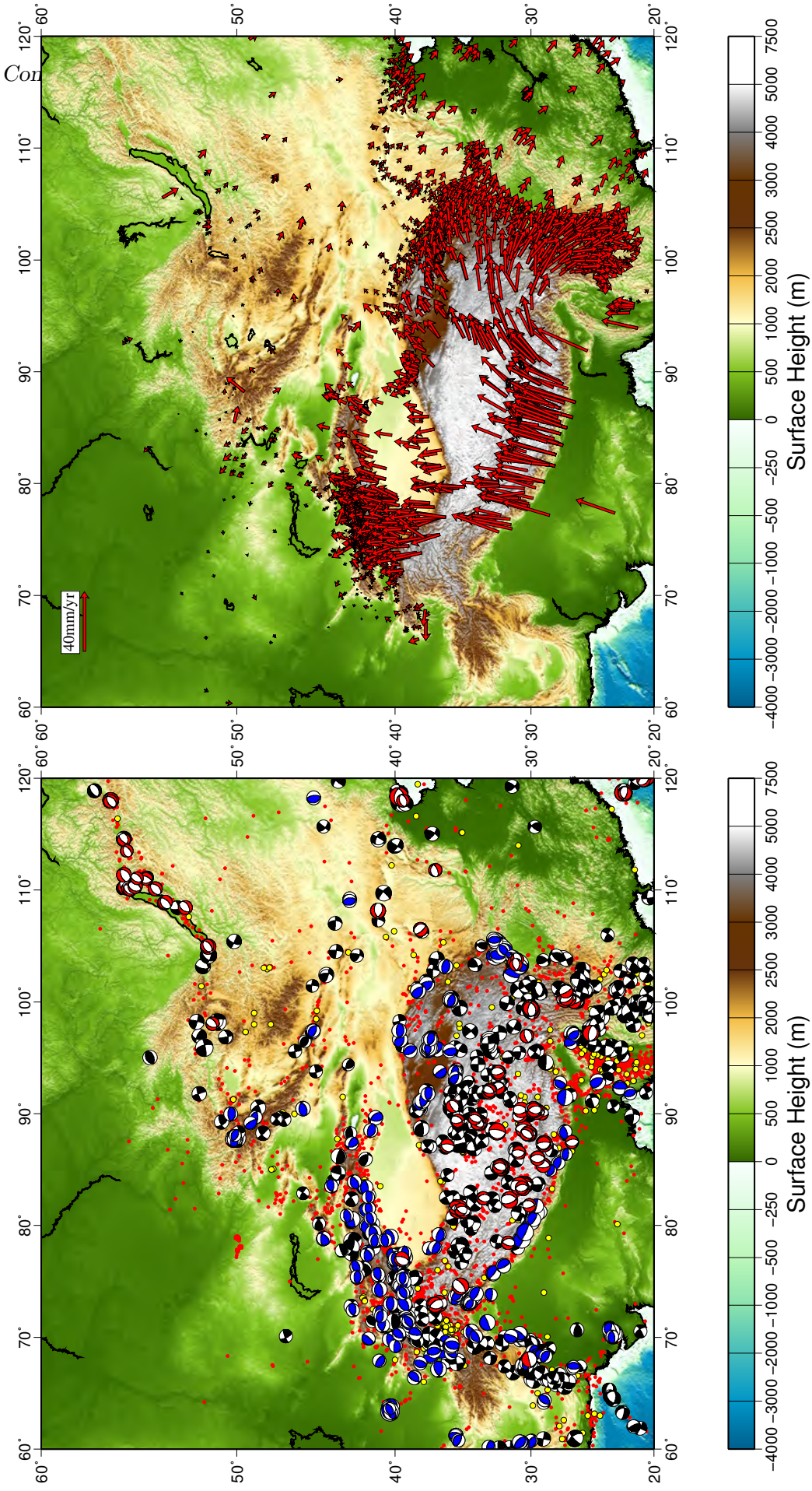
Figure 2: Left Panel: Seismicity of Asia. Focal Mechanisms are for earthquakes of magnitude greater than about 5, from the GCMT catalogue [*http://www.globalcmt.org*]. Red dots are the epicentres of earthquakes greater than magnitude 4 since 1964. **Left Panel:** Velocities of GPS sites relative to Eurasia [*Calais et al.*, 2006; *Gan et al.*, 2007; *Zubovich et al.*, 2010].
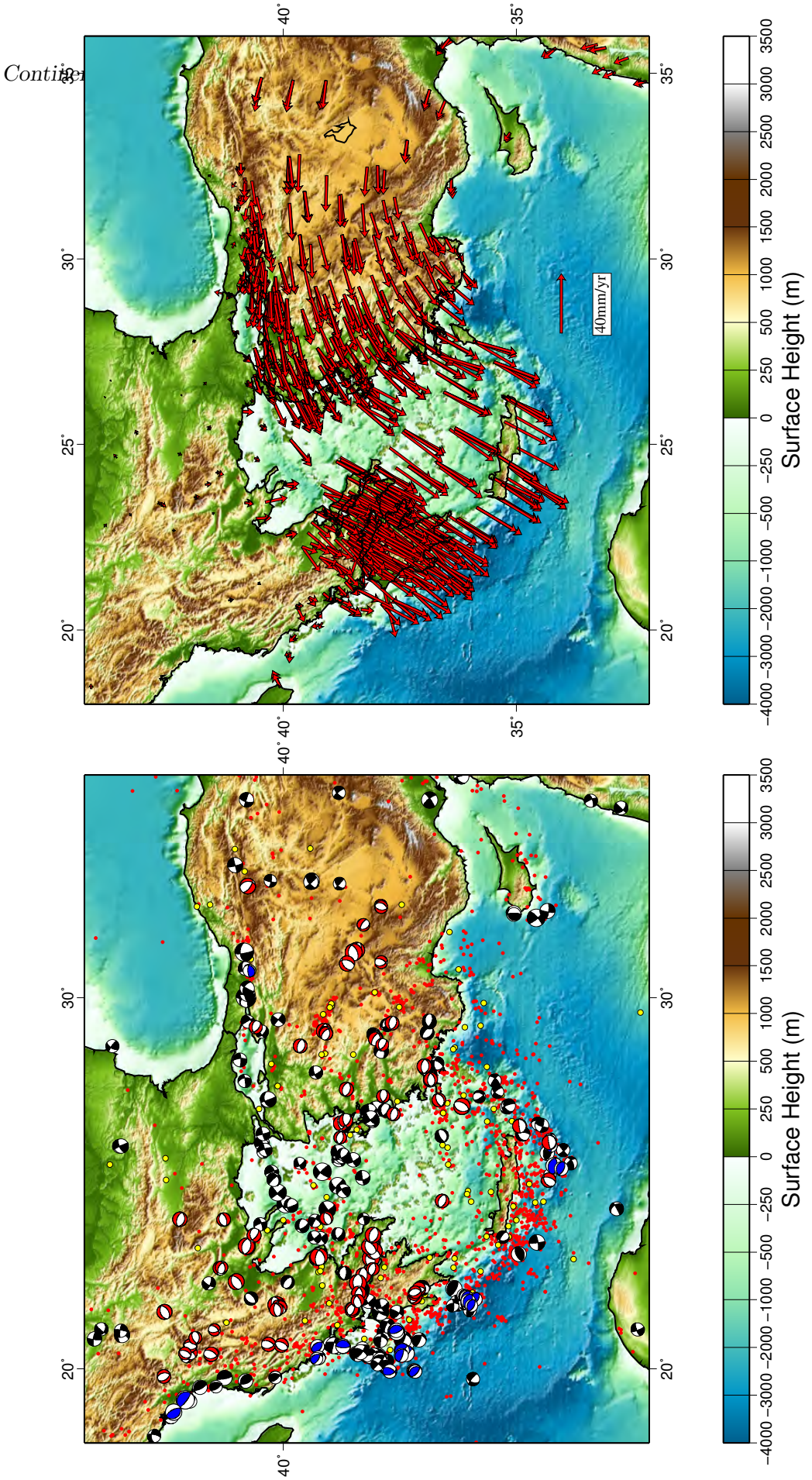
Figure 3: As for Figure 2, but for the Aegean. GPS vectors are from *Nocquet* [2012].
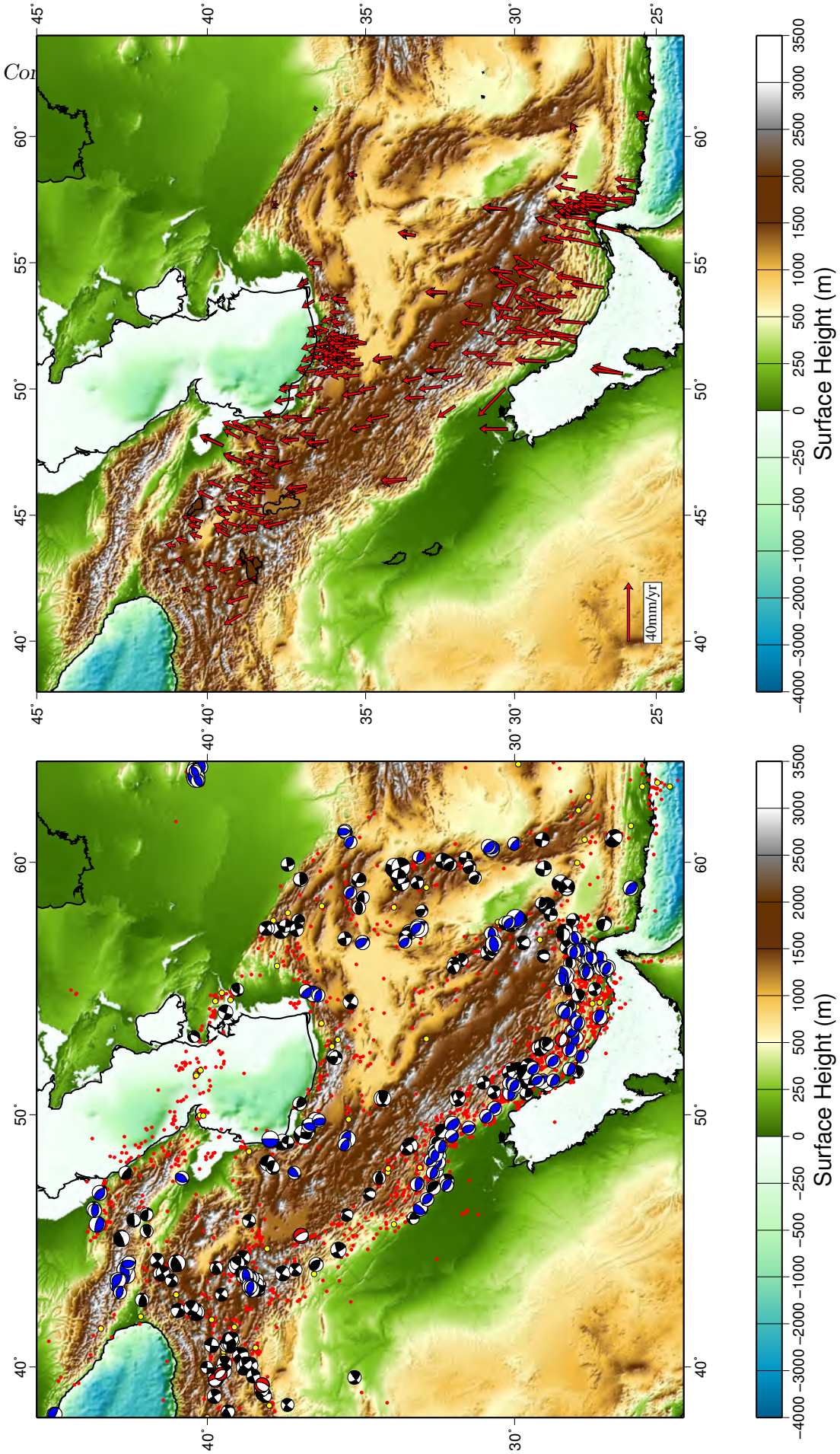
Figure 4: As for Figure 2, but for Iran.
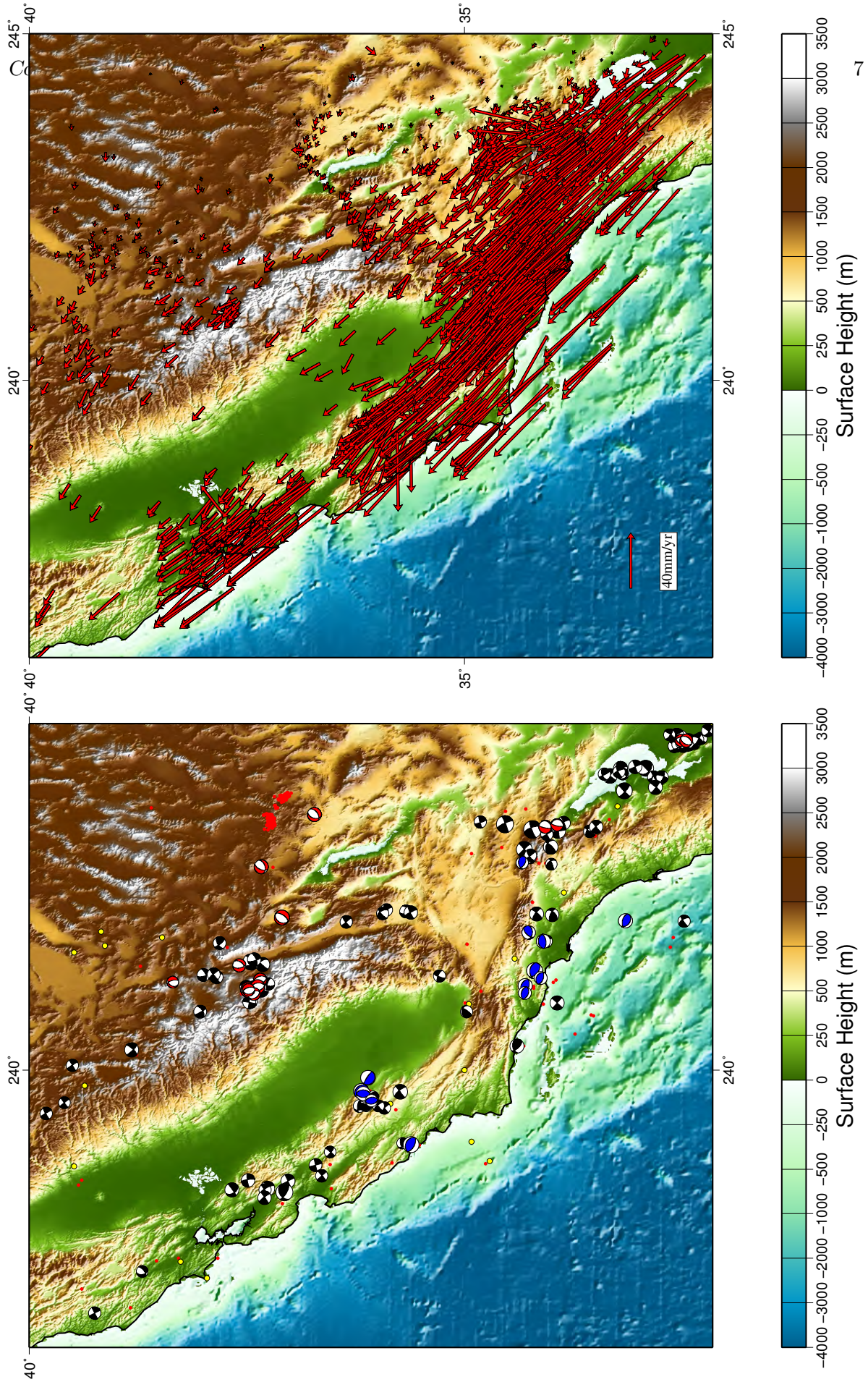
Figure 5: As for Figure 2, but for California. Arrows show velocities relative to North America; SCEC velocity field.
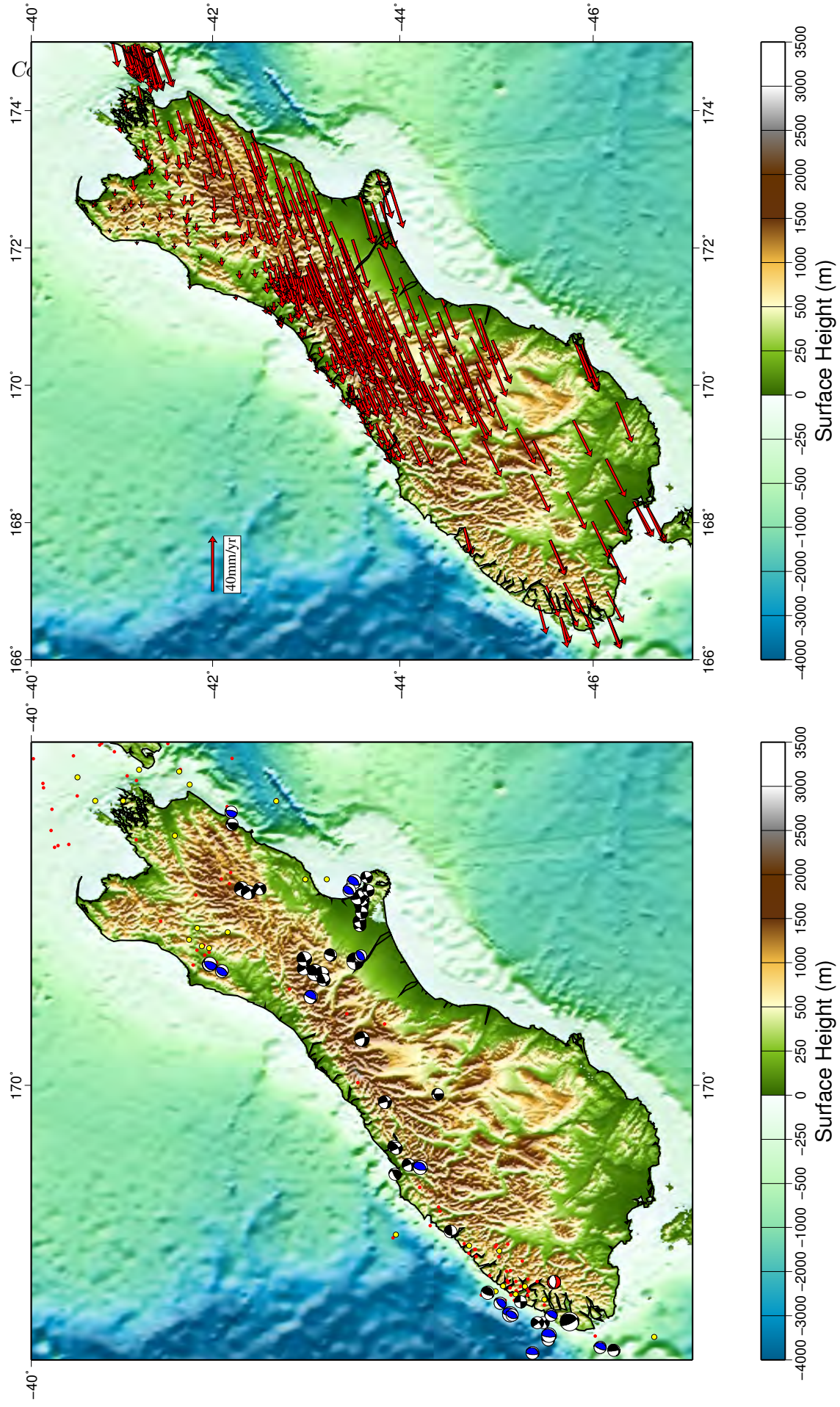
Figure 6: As for Figure 2, but for the South Island of New Zealand. GPS vectors show motions relative to the Australian plate [*Wallace et al.*, 2007].

8

Scales of Deformation on the Continents

There are three obvious divisions to the continental lithosphere: the seismogenic upper crust, the entire continental crust, and the lithosphere as a whole.

Seismogenic crust

Seismicity in continental crust often shows an abrupt cut-off in activity in the depth-range of 10–20 km. The depth of this cut-off varies from place to place, but it is usually possible to identify such a cut-off within the middle crust. Within the seismogenic layer, an important fraction of the deformation takes place by frictional sliding on faults, giving rise to earthquakes. Study of these earthquakes has been a major source of information on the kinematics of active continental deformation. As we discuss later, there are reason to believe that we can obtain an accurate picture of the kinematics of this layer, at the scale of its own thickness – 10–20 km.

The crust as a whole

The continental crust varies greatly in thickness and surface height, particularly in zones of active deformation. To a good approximation, surface elevation contrasts whose horizontal scale exceeds about 100km are compensated isostatically. Isostatic balance is, however, a state of balance of vertical forces; isostatically balanced columns can differ in their gravitational potential energy, and therefore have the potential to do work on each other. Contrasts in gravitational potential energy contribute importantly to the dynamics of the continents; for example they are responsible for the active east-west extension of the Tibetan plateau, immediately to the north of the compressional boundary of the Himalaya.

The lithosphere

The third layer is the lithosphere itself. In plate tectonics' terminology the term 'lithosphere' has often been equated with the term 'plate', with some confusion, because a plate does not strain, except in a small elastic way. The continental lithosphere obviously does deform, and by large strains. Other uses of the term 'lithosphere' have seismological, petrological, thermal, or mechanical connotations. We shall be investigating the forces responsible for continental deformation and shall, therefore, use the term 'lithosphere' to refer to the mechanical boundary layer at the top of the mantle. To deform this layer at geological strain rates requires stresses that greatly exceed the stresses involved in mantle convection. It is difficult to be precise about either how great these stresses must be, or about how thick is the layer that supports them. Several lines of argument suggest that the upper 60–100 km of the continental lithosphere may be capable of supporting deviatoric stresses of 10–100MPa over geological time-spans.

Deformation delineated by seismicity and topography

Eurasia converges, along its southern boundary, with the African, Arabian, and Indian plates; the seismicity in southern Europe and the Middle East stretches for about 2000 kilometres

along strike and for 500–800 km across strike (Figures 3, 4). In southern Asia (Figure 2) the seismicity covers an even larger area. All the earthquakes depicted in these figures had focal depths shallower than 10–20 km and, with the exception of thrust-faulting earthquakes around the Hellenic trench (18ºE–30ºE, ∼34ºN), all occurred within continental crust.

The earthquakes are closely correlated, spatially, with regions where the surface lies either considerably above or considerably below the elevation of undeforming continental lithosphere. This variation in surface heights implies variation in crustal thickness, and thus strain of the crust. In some regions the strain implied by the crustal thickness is consistent with the active deformation. For example, thrust faulting in the Zagros mountains, or the Himalaya, could have produced the thickened crust in those regions within a few million years. Equally, the extensional faulting in the Aegean could have reduced crust of normal thickness to the present thinned crust of the region.

In other regions, however, the active faulting could not have produced the present distribution of topography, starting from crust of normal thickness. This is most obvious in Tibet, where the surface elevation is about 5km, and the crustal thickness is in excess of 60 km. The entire plateau is deforming by a combination of strike-slip and normal faulting (Figure 2), implying horizontal extension and crustal thinning.

The Bare Bones of Faults and Earthquakes

What is a fault?

A **fault** is an approximately planar surface in a body of rock, across which observable relative motion of the rock has occurred. The orientation of a fault is specified by its *strike* and *dip*. The strike is the angle between the trace of the fault on the earth's surface, and the north. The dip is the angle between the plane of the fault and the horizontal.

The relative motion of the rocks on either side of the fault is called the **slip**. Faults are classified according to the sense of slip. If the sense of slip is parallel to the strike of the fault, the fault is called a **strike-slip fault** (Figure 8). The relative motion across strike-slip faults is horizontal. An observer facing a strike slip fault will see either that the rocks on the other side have moved to the left or that they have moved to the right. Strike-slip faults are called *right-lateral* or *dextral* if the sense of relative motion is to the right, and *left-lateral* or *sinistral* if the sense of motion is to the left (Figure 8). (A moment's thought should convince you that the sense of motion does not depend on which side of the fault you observe.)

If the sense of slip is predominantly in the direction of dip, then the fault is called a **dip-slip fault**. The rock lying above a dip-slip fault is known as the **hanging wall** and the rock below is called the **footwall**. If the sense of slip shows that the hanging wall has moved downwards with respect to the footwall the fault is called a **normal fault**. If the hanging wall has moved up with repsect to the footwall, then the fault is called a **reverse fault** (Figure 8). Reverse faults whose dips are shallower than about 20° are commonly referred to as **thrust faults**.
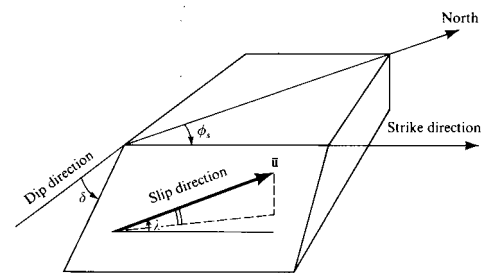
Figure 7: Convention for describing slip in an earthquake; a right-handed system, standing on the footwall and facing the fault. The slip direction shows the direction of motion of the hanging wall relative to the footwall, and is measured by the rake, λ, which is the angle *in the fault plane* between the strike direction and the slip vector. For the trigonometrically inclined, the slip direction ϕ_{slip} can be calculated from the dip, δ, rake, λ, and strike, ϕ_{s} by: $\phi_{\text{slip}} = \phi_{\text{s}} + \arctan\left(-\sin\lambda\cos\delta/\cos\lambda\right)$.
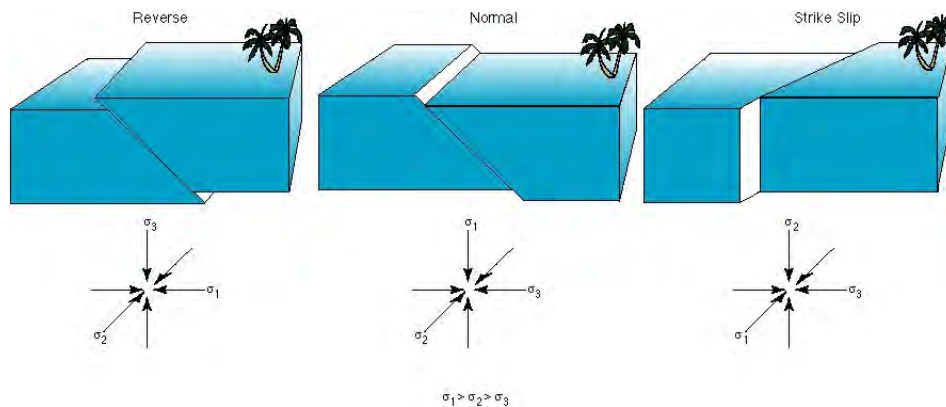
Figure 8: fault types and their relation to the state of stress. The arrows show the directions of the maximum compressional stress, σ_1, the smallest compressional stress, σ_2,

A fault that has slipped in historical time (*e.g.*, past 10,000 years) or recent geological time (*e.g.*, past 500,000 years) is said to be **active**.

What is an Earthquake?

The modern understanding of earthquakes is due to H.F. Reid, who investigated the 1906 earthquake that devastated San Francisco[1]. Many people think of earthquakes as the cause of strain. Reid's great insight was to recognise that earthquakes are the *result* of slow elastic strain of the earth. This strain accumulates over decades or centuries until an earthquake releases it in a few seconds or minutes.

Imagine slowly bending a ruler. The ruler can be bent into an arc, but eventually, if it is bent far enough it will snap. While it is bending, the ruler strains elastically. At the instant of snapping, the elastic strain in the ruler is released. After it has snapped the ruler is in two separate parts, each of which is straight. Reid's suggestion, which is now widely accepted as the explanation for earthquakes, is that the crust of the earth deforms slowly between earthquakes, and that each earthquake represents rapid slip of the two sides of a fault past each other (Figure 9). As the fault slips, the crust on either side straightens. This idea is known as **elastic rebound**.
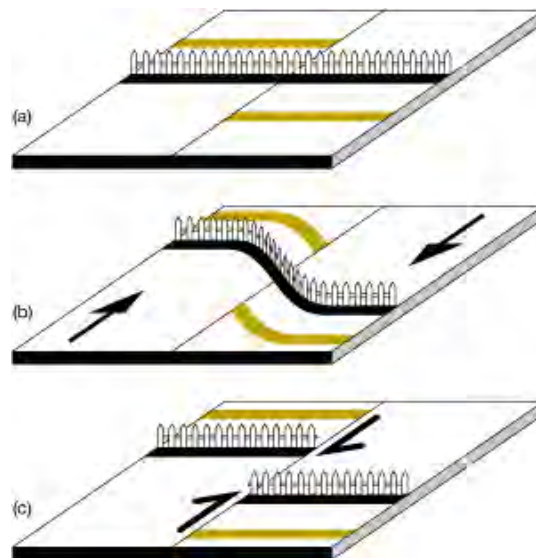
Figure 9: Distortion of the crust (and a fence built on top of it) during a cycle of build-up of strain and its release in an earthquake. a) A fence is (re)built in a straight line, immediately after the last earthquake. b) Under the action of distant forces, the crust slowly deforms; this is known as the *interseismic* period. c) The strain of the crust is released by slip on the fault; leaving the fence, and perhaps other structures, in a state of disrepair.

The size of an earthquake

The correct measure is the *Seismic Moment Tensor* **M** (see Figure 7):

$$M_{ij} = M_0(\hat{u}_i \hat{n}_j + \hat{u}_j \hat{n}_i) \tag{2}$$

$$
\begin{aligned}
M_0 &= \mu A s \quad \text{(scalar moment)} \\
A &: \quad \text{area of fault plane} \\
s &: \quad \text{average slip} \\
\mu &: \quad \text{shear modulus} \\
\mathbf{\hat{u}} &: \quad \text{unit vector in direction of slip} \\
\mathbf{\hat{n}} &: \quad \text{unit vector normal to fault plane}
\end{aligned}
$$

---

[1]This is what the textbooks say. In my view the same claim can be made for R. D. Oldham of the Geological Survey of India, who made equivalent observations after the 1897 Assam earthquake. Like Reid, Oldham suggested that the idea of elastic rebound could be tested by geodetic measurements. Unlike Reid, he has the misfortune that an unacceptable fraction of the people who tried to make his proposed measurements were eaten by tigers. Oldham had the consolation of later discovering the Earth's core.

The **Moment magnitude** of an earthquake is given by:

$$M_{\mathrm{w}} = \frac{2}{3}\log_{10}(M_0) - 6.1$$

with M_0 measured in **N m**.

Moment- (or magnitude-)frequency relation

Large earthquakes are much less frequent than small earthquakes (roughly a factor of 10 for each unit of magnitude Figure 10).

Many observations, local, regional, and global lead to the conclusion that there is a relation between the size and the frequency of earthquakes of the kind:

$$N(M_0) = aM_0^{-b} \tag{3}$$

where N is the number of events having moment greater than or equal to M_0 in a given time interval. The value of b is found to be about $2/3$.
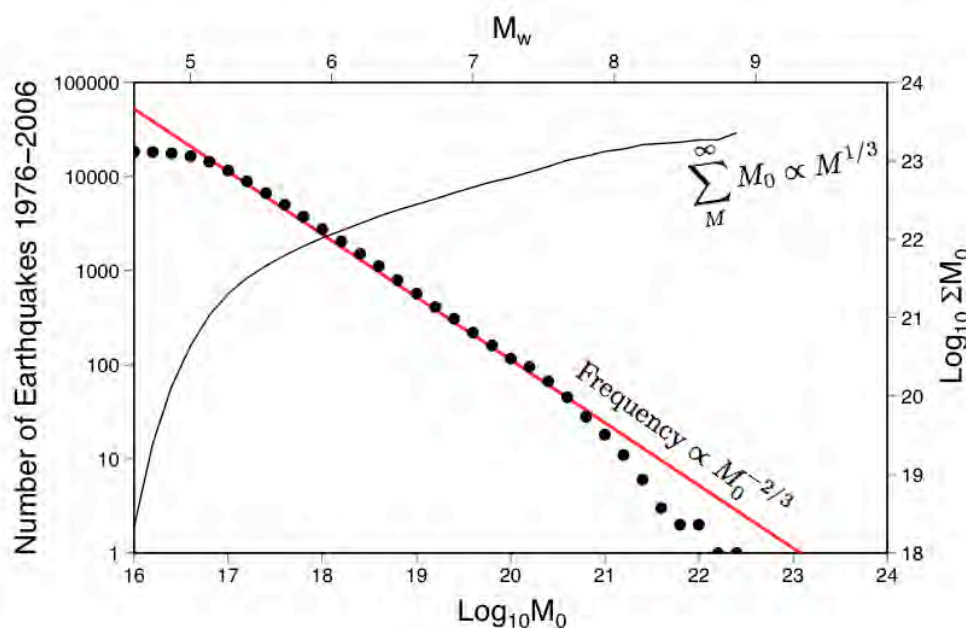
Figure 10: Moment-Frequency relationship for global earthquakes (dots, number of earthquakes above a given moment, see left-hand vertical axis). Solid curve shows cumulative moment release in all earthquakes having moments upto a given value of M_0 (right-hand axis): note that the largest earthquakes account for most of the moment release.

In any given region, there will always be earthquakes that are too small to measure. The relation (3) allows one to estimate what fraction of the seismic moment is released in unobserved earthquakes. Rewrite (3) as:

$$N(M_0) = \int_{M_0}^{\infty} n(M)\mathrm{dM} \tag{4}$$

where

$$n(M) = -\frac{dN}{dM} \tag{5}$$

is the 'density' of events of a given moment, M_0. Suppose that in a particular region, the maximum observed scalar moment is M_{max}, and the minimum moment for which a reliable moment tensor can be determined is M_{min}. Then the total moment release over the interval of observation is

$$M_{\mathrm{tot}} = \int_0^{M\mathrm{max}} M\ n(M)\ \mathrm{dM} \tag{6}$$

whereas the total observed moment release is:

$$M_{\mathrm{obs}} = \int_{M_{\mathrm{min}}}^{M\mathrm{max}} M\ n(M)\ \mathrm{dM} \tag{7}$$

So:

$$\frac{M_{\mathrm{obs}}}{M_{\mathrm{tot}}} = 1 - \left(\frac{M_{\mathrm{min}}}{M_{\mathrm{max}}}\right)^{(1-b)} \tag{8}$$

Because the instrumental period of earthquake observation is short (about 100 years), whereas the repeat time for large earthquakes may be much longer than this, it is always possible that M_{max} in a particular period of observation may be substantially smaller than the moment of the largest earthquakes that ever occur in the region. The relation (8) allows one to estimate the degree to which long-term seismic strain is underestimated in this case.

Equation (8) also shows that, although large earthquakes are less frequent than small earthquakes, the large earthquakes account for the majority of the seismic moment release.

Scaling relations for earthquakes and Faults.
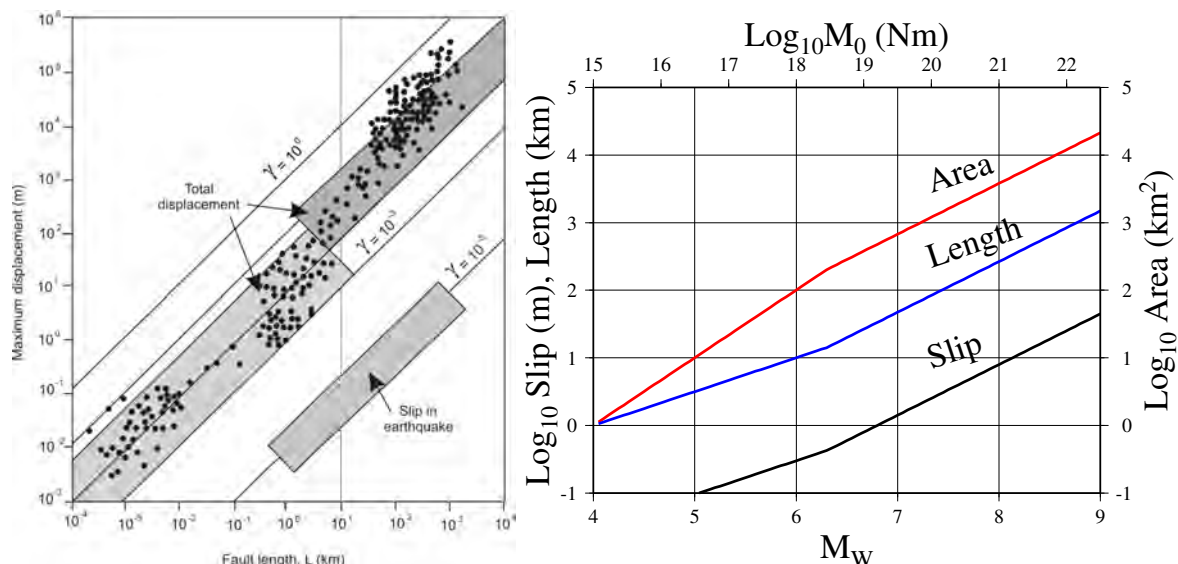
Figure 11: Left Panel: (From *Cowie and Scholz* [1992].) Displacement-to-length ratios (γ) on faults. For incremental slip on faults in earthquakes γ is typically $1 - 10 \times 10^{-5}$. For total cumulative offsets on faults, γ is more scattered and in the range 10^{-1} to 10^{-3}. Note the apparent change in γ near 10 km length, which corresponds to the break between 'big' and 'small' faults. **Right Panel:** Area, length, and Slip for earthquakes of different magnitudes.

- The length and amount of slip in an earthquake both scale with the moment: The slip in an earthquake is about 3×10^{-5} the magnitude of the fault length.

- Most of the damaging earthquakes on the continents rupture through the entire depth of the upper crust (10–20 km).

- The moment of an an earthquake is proportional to the area of the fault that slipped multiplied by the amount of the slip, so if you know how long a fault segment is, you can make a pretty good estimate of the size of earthquake it is capable of generating. Short faults can't generate large earthquakes, and it would be unwise to assume that a long active fault will *not* generate a large earthquake at some time (Figure 11). Although, in general, most of the strain that accumulates on a fault will eventually be released by the largest earthquake, there may well be many small earthquakes in the interseismic period, and there are always many aftershocks after a large earthquake.

- The total offset on a fault scales differently from the offset in an individual earthquake: it is about 10% of the magnitude of the fault length. One consequence of this scaling is that faults must, in general, increase their length as they increase their cumulative offset.

Intensity

The figures below show the distribution of ground shaking associated with four recent prominent earthquakes. (See Glossary for definitions of the Intensity levels). The figures illustrate how the Intensity depends on distance from the earthquake, and the size of the earthquake. Together with the death tolls of the earthquakes, these figures also emphasize the roles of proximity to the earthquake, and vulnerability of building stock in determining the level of fatalities.
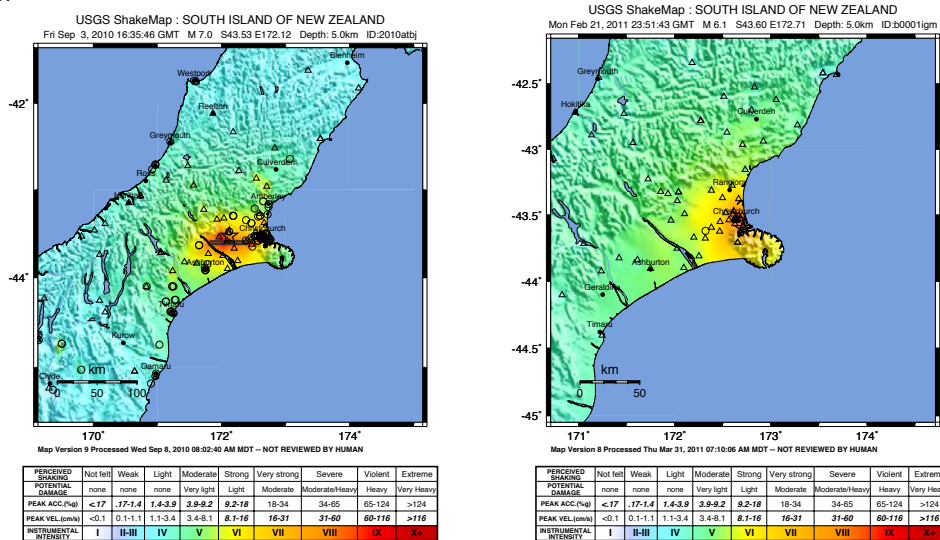
Figure 12: Size matters, but position matters more. **Left:** Intensity of ground shaking due to the Fri Sep 3, 2010 M 7.0, Darsbury earthquake. No deaths. **Right:** Intensity of ground shaking due to the Mon Feb 21, 2011 M 6.1, Christchurch earthquake. 183 deaths. (http://earthquake.usgs.gov/earthquakes/eqinthenews/)
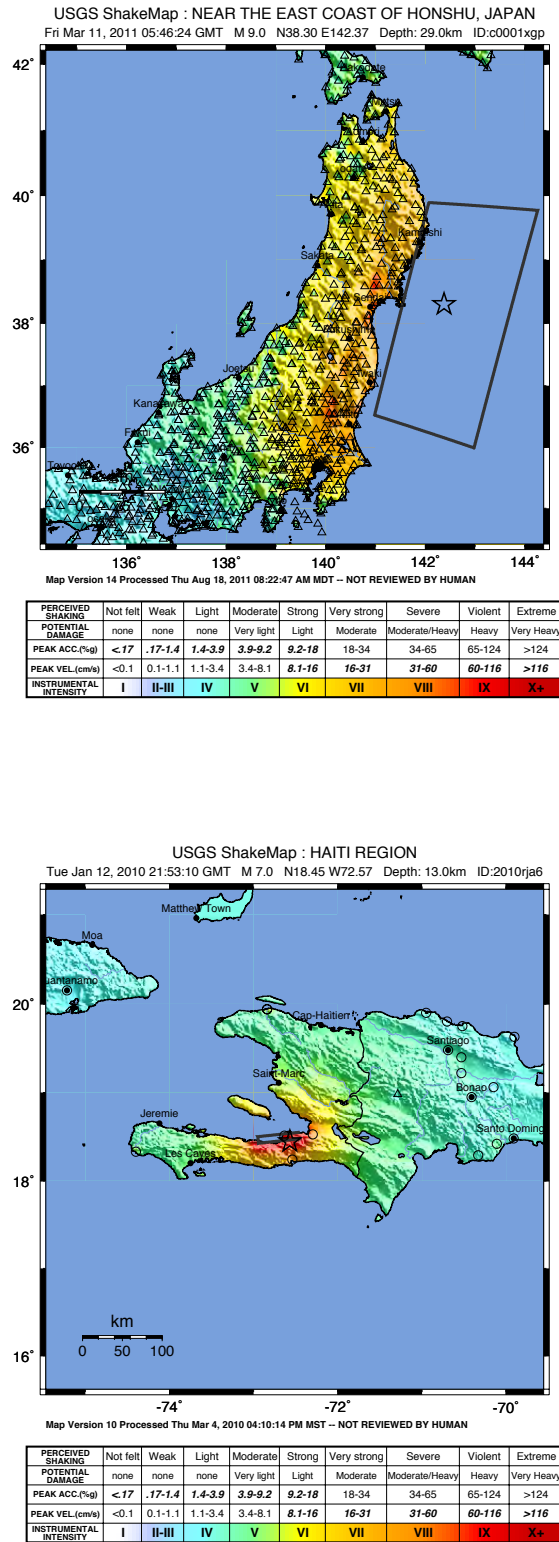
Figure 13: Size matters, but vulnerability matters more. **Left:** Intensity of ground shaking due to the Fri Mar 11, 2011 M 9.0 Tohoku earthquake. About 1,000 deaths from building collapse; 20,000 from the tsunami. **Right:** Intensity of ground shaking due to the Tue Jan 12, 2010 M 7.0, Haiti earthquake. 100,000–200,000 deaths.

Fault plane solutions

Imagine that you were standing close to the epicentre of a strike-slip earthquake, perhaps the 1906 San Francisco earthquake. The very first motion that you felt from the earthquake would be made by the P wave travelling from the hypocentre. (P waves are much smaller than the surface waves, so anyone standing close enough to an earthquake to feel a P-wave would also experience a large amount of shaking in all directions as the surface waves rolled by. We are talking about *only the first motion* felt by an observer.) You would feel the first motion of the ground as towards you (away from the hypocentre), or away from you (towards from the hypocentre), depending upon where you were standing relative to the fault (Figure 14). We may imagine a large number of observers scattered around the fault, and we could shade the ground around the fault according to whether the observers felt the first ground motion as away from them or towards them. We can see that there is a simple pattern to these observations; they separate into four quadrants that are separated by the fault, and by another plane at right-angles to the fault and passing through the hypocentre (Figure 14). We must emphasise that this construction treats the earthquake as though it occurred at a point, whereas in reality it ruptures a plane of finite size. Except for the largest earthquakes, this complication does not usually cause difficulty.
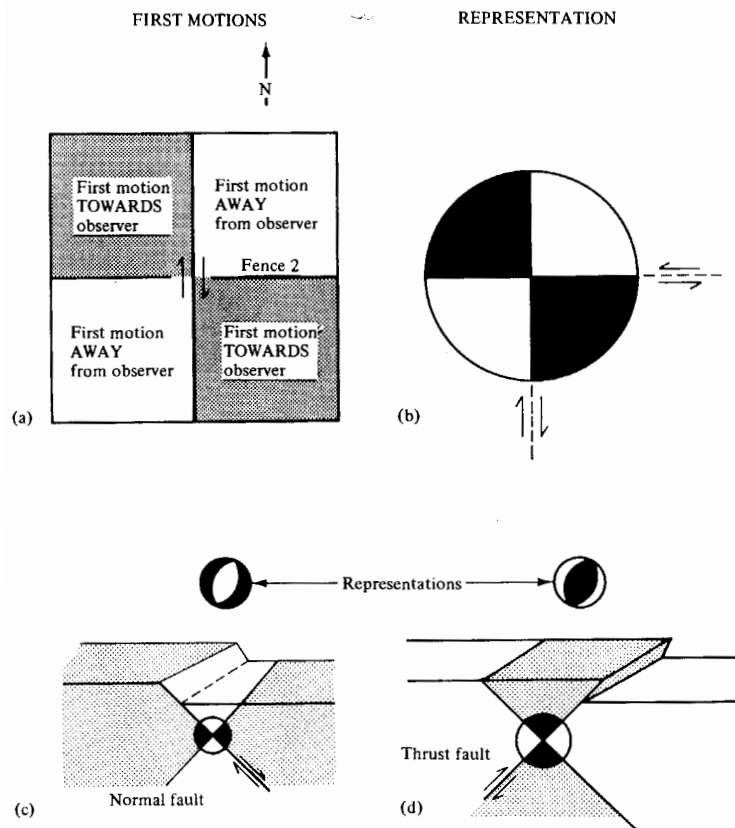
Figure 14: Ground motion near a strike-slip earthquake. a) The ground motion in the neighbourhood of the fault. Regions where the first motion is towards the observer are shaded. b) A representation of the focal mechanism of an earthquake. A transparent hemisphere lies beneath the earthquake, with its centre at the hypocentre. The surface of the hemisphere is shaded according to whether the ray passing through the surface has first motion towards the observer, or away. The hemisphere is viewed from on top. c) d) Focal mechanisms for dip-slip faults.

We have so far imagined only the distribution of motions that human observers might feel if they were close to the earthquake. Seismometers are far more sensitive than people, and any earthquake larger than about magnitude 5 can be measured by a seismometer even if it is at the far side of the earth. The pattern of observations in Figure 14 is as valid for seismic waves travelling to the far side of the earth as it is for the nearby observer. Of course, P waves travelling to the far side of the earth do not travel along the surface, but take off downwards into the earth.

The seismologist makes the link between the pattern shown in Figure 14 and the observations made at distant seismic stations by imagining that a large transparent hemisphere underlies the earthquake (Figure 14), and then shading each part of that hemisphere according to whether the seismic ray passing through it has a first motion towards the seismometer, or away – just as we imagined shading the land surface near the epicentre (Figure 14). Viewed directly from on top, the hemisphere looks exactly the same as the picture of the near-surface displacements in Figure 14).

So far we have only drawn the pictures for a strike-slip earthquake. The patterns of waves leaving other types of earthquakes are different – but only because of the different orientations of the faults, in all other respects the arguments remain the same. So, for example, a normal fault would show a pattern in which most of the waves taking off downwards would have first motions away from the observer (Figure 14c), whereas thrust faults show to opposite pattern (Figure 14d).
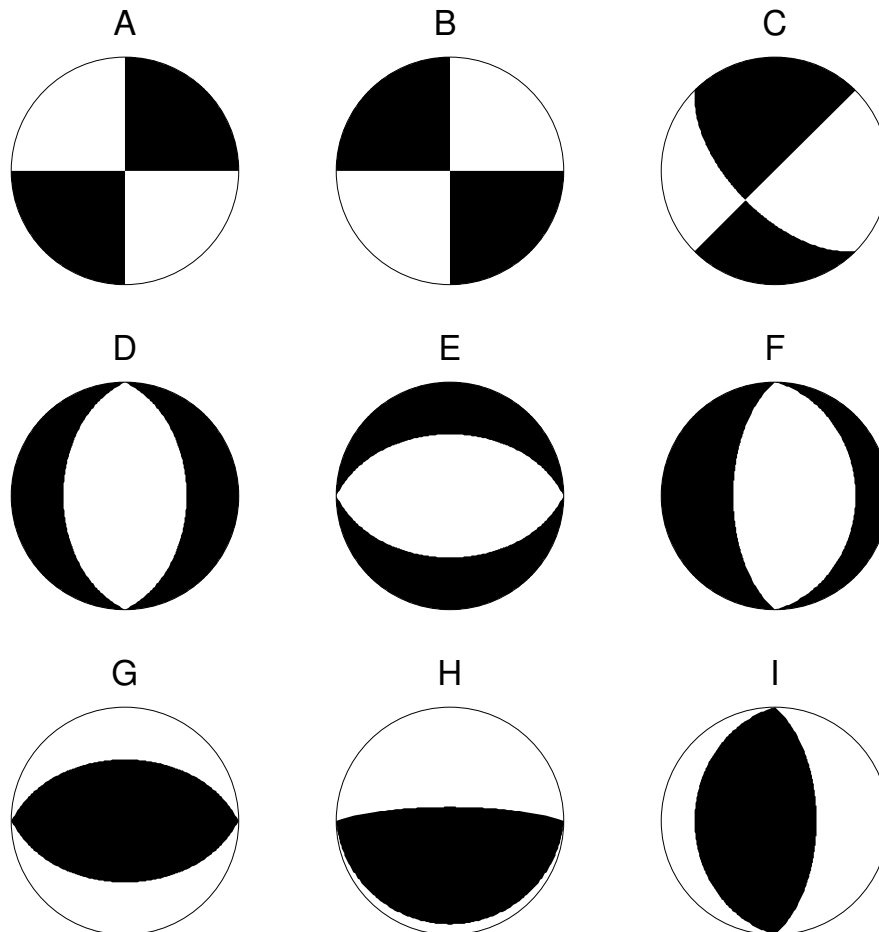
Figure 15: Focal mechanisms (lower focal hemisphere projections) for strike-slip-, normal-, reverse-, and thrust-faulting earthquakes.

A Strike (S) 180º, dip (δ) 90º, rake (λ) 0º: A North-south, left-lateral strike-slip fault, but the focal mechanism is equally compatible with an east-west right-lateral fault. (The ambiguity will not be repeated for the other faults, and it is a good idea for you to try to work out the other possible fault for yourself.

B S 180º, δ 90º, λ 0º Work out fault type from **A**

C S 135º, δ 60º, λ 0º A dipping fault with pure strike-slip motion; the other plane is a vertical fault with a small amount of oblique slip (which sense?).

D S 180º, δ 45º, λ -90º North-south normal fault dipping W.

E S 90º, δ 45º, λ -90º Work it out

F S 180º, δ 60º, λ -90º Normal fault dipping at 60º.

G S 90º, δ 45º, λ 90º Reverse fault, striking east and dipping (which way?).

H S 90º, δ 10º, λ 90º Thrust fault, dipping which way?

I S 180º, δ 30º, λ ??

Earthquake seismology

Seismology contributes to tectonic geology mostly through earthquake source studies or, more specifically, through being able to estimate the location, geometry and size of slip on faults. Earthquake source parameters are routinely reported by various agencies and easily accessible on-line. They are widely quoted in geological and engineering applications, often with little appreciation of their limitations. This section provides a short summary of their capabilities and pitfalls that may be helpful to those who are not professional seismologists.

1. *Locations*

Routinely reported locations of earthquakes by agencies such as the United States Geological Survey (USGS) or International Seismological Centre (ISC) are based on arrival times of P waves at seismic stations round the globe. The location accuracy depends critically on the distribution of stations around the epicentre and especially on the presence or absence of close stations. Within dense local networks, where the station spacing is comparable with the earthquake focal depth (typically 10–15 km on the continents), and with the inclusion of S waves as well as P, location accuracies can reach 1 km or better, and depend mostly on uncertainties in the crustal velocity model. But this is rarely the situation outside places like California and Japan. In most continental regions there are sparse station networks and locations are based mainly on arrivals at teleseismic distances (> 30º). In these circumstances the poor station geometry and the assumed Earth velocity model (which is always spherically symmetric) can lead to location errors of tens of kilometres. For earthquakes that occurred prior to about 1960 the errors can often be 100 km or more. These errors tend to decrease with time towards the present as the number of seismic stations has increased, but even for a well-recorded modern earthquake the location error can be 10–15 km.

The best global catalogue is probably that known as the EHB Bulletin, now maintained by the ISC (www.isc.ac.uk/ehbbulletin)and named after the algorithm and approach of *Engdahl et al.* [1998], who relocated 100,000 events between 1964 and 1995 (and have since updated this database). They used other phases in addition to P as well as an improved global velocity model, and their catalogue is complete down to about M_w 5.2. Their revised locations are certainly improvements, especially in oceanic regions and for deep earthquakes, but are not likely to remove the epicentral errors of ∼10–15 km outside dense regional networks, as these errors arise from the station geometry and the inadequacies of a spherically symmetric Earth model. To put this in perspective, 10–15 km is the expected length of a fault that moves in an earthquake of ∼M_s 6.0, so the location error could easily lead to an apparent association of the earthquake with the wrong fault.

2. *Focal depths*

Earthquake focal depths are a special problem. When based on arrival times alone, they are much less well determined than the epicentre because of a trade-off between the depth and origin time in the location procedure. Depths reported in routine bulletin locations can be wrong by 50 km or more, even for well-recorded earthquakes, and are for this reason sometimes fixed at an arbitrary depth (in the past and by tradition, often 33 km for the USGS and ISC). In spite of this being a well-understood problem, inaccurate focal depths reported in bulletins are often taken at face value and misinterpreted. For example, earthquakes apparently at depths

of ∼100 km beneath the Zagros mountains of SW Iran have, in the past, been attributed to subduction of Arabia beneath Iran, whereas there is no real evidence for any earthquakes deeper than about 20 km in that region. In reality, such bulletin locations are unable to distinguish whether the earthquake was in the crust or the mantle, let alone whether it was in the basement rather than the sedimentary cover.

Once again, the EHB Bulletin is a partial improvement, because it attempts to use other phases, such as the surface reflections pP and sP, in addition to P. For earthquakes that are genuinely deeper than about 50 km the direct and reflected phases are clearly separated in time and the focal depth is certainly better resolved. But this catalogue still puts many earthquakes in the continental mantle that are likely to be within the crust, probably because the surface reflections are rarely clear for shallow events and can be misidentified.

There are two ways around this problem. With dense local networks the depth can be resolved to within a kilometre or so. Otherwise the solution is to analyse the shape of the P and S waveforms themselves and to constrain the depth with synthetic seismograms. This is possible for earthquakes of $M_s >\sim 5.5$ and is relatively routine, but time consuming. It is discussed below (section 4).

3. *Fault plane solutions*

Earthquake fault-plane solutions describe the orientation of the fault (its strike and dip) and the direction of the slip vector within its plane (the rake, see Figure 7). They can be determined from the observed polarities of P wave onsets, which can be towards or away from the hypocentre. Such determinations are called 'first-motion' fault-plane solutions, and were used in the 1960s to demonstrate the rigidity of the oceanic plates and the nature of plate boundaries. Fault-plane solutions are described by two orthogonal planes in space, one of which is the fault plane and the other is the plane to which the slip vector is the normal. These ('nodal') planes define four quadrants that separate the first motion polarities of the P wave radiation pattern. They are usually plotted as lower hemisphere stereographic projections, and their construction is described in all seismology text books (Figure 14). An important property of this seismic radiation pattern is that it cannot, alone, be used to distinguish which of the two orthogonal nodal planes is the fault plane. This ambiguity is best resolved by additional information, such as surface faulting or the aftershock distribution.

The accuracy of first-motion fault-plane solutions depends again on the station distribution and the consistency of the observed polarities. First motions are best read on long-period instruments, where the noise is less, but this effectively restricts our ability to construct them to earthquakes of about m_b 5.5 or larger, except with dense local networks. Proper evaluation of the reliability of fault plane solutions requires a scrutiny of the observed polarity distributions, which, in reputable works, are published alongside the solutions themselves. Better estimates of earthquake source parameters can now be made using waveform modelling (discussed below), but first motion solutions remain an important historical database and are still the best way of determining the mechanisms of small events using local networks.

4. *Source parameters from waveform modelling*

With the advent of synthetic seismogram techniques in the 1970s, various methods are now used to estimate earthquake source parameters from the waveforms themselves, rather than

from just the polarity or arrival time of the first motions. Some of these methods have become routine and, in particular, a catalogue of earthquake source parameters is available from the Global Centroid-Moment-Tensor (CMT) Project [*http://www.globalcmt.org*] that is complete for all earthquakes larger than $M_w \sim 5.5$ back to 1977. This is an extraordinary resource of immense value in seismology, tectonics and engineering, but is often used without much thought to its limitations. A brief discussion of what waveform analysis can achieve may help the non-professional user.

The most widely-used methods of waveform inversion involve either a simplified ray theory approach [*e.g. McCaffrey and Nábělek*, 1987] or normal mode summation [*Dziewonski et al.*, 1981]. The ray theory approach typically analyses just the early part of the P and SH (the horizontal component of S) waveforms, and is commonly referred to as 'body-wave' analysis, while the normal mode approach is often referred to as 'centroid moment tensor' or 'CMT' analysis. Both approaches attempt to use wavelengths that are long compared to the source (fault length) of the earthquake, so that the source appears as a conceptual point in space (the 'centroid') even though it may have a finite duration in time. In principle the centroid then represents a weighted average or centre of the rupture surface, and if the rupture breaks the Earth's surface it may extend an approximately equal distance below the centroid depth.

In practice, the body-wave and CMT approaches have differences that are significant. Most body wave inversions explicitly assume a double-couple source (slip on a fault), and because they look at only a short window of data (typically 20–40s for shallow earthquakes) can afford to look at relatively high frequencies. A favourite frequency range is that offered by the old WWSSN 15-100s long-period instruments, with a peak response at around 15s period. Since the P wave velocity in the crust is ~ 6 km s^{-1}, this is sufficiently long-period for the sources of most moderate-sized earthquakes ($M_s \sim 5.5$–6.8) to look simple and for complications arising from geological structure near the source and receiver to be relatively unimportant. On the other hand, enough high frequency is retained for the waveforms to be sensitive to source depth for shallow earthquakes, as the time separation between P and pP and between P and sP (typically around 4–10s for depths of 10–20 km) can be resolved. For earthquakes larger than $\sim M_s$ 6.8 the approximation of a point source often breaks down at these periods and the waveforms commonly exhibit the character of a multiple source with several discrete sub-events. These can usually be modelled satisfactorily by a series of separate centroid sources distributed in space and time [*e.g. Haessler et al.*, 1992]. For large strike-slip events the direction of propagation can sometimes be determined in the same way, thus resolving the ambiguity between the nodal planes in the fault plane solution [*e.g. Berberian et al.*, 1999].

In contrast to the body wave techniques, the CMT methods usually solve for the six independent elements of the centroid moment tensor, which is an alternative description of the seismic source in terms of a 3×3 symmetric tensor whose eigenvectors are related to the source orientation and whose eigenvalues are related to its size [see *e.g. Shearer*, 1999]. CMT inversions usually assume no volume change (i.e. that the trace of the moment tensor must be zero) but do not require that the source represents slip on a fault (called a 'double-couple' source, which would require one eigenvalue of the moment tensor to be zero). The CMT methods usually use a much longer time window of data than the body-wave techniques and to make the inversion manageable they generally low-pass filter the data, typically at ~ 0.022 Hz (45s period) for the Global CMT (gCMT) solutions [*e.g. Ekström et al.*, 2012]. This has two important consequences. One is the relative insensitivity of the CMT inversion to the components of the moment tensor that correspond to dip-slip on vertical or horizontal planes for shallow events,

which translates into a relatively large uncertainty in the dip of nodal planes for normal or thrust fault solutions. A second consequence is the inability to resolve the centroid depth for events shallower than about 30 km. For this reason the Global CMT catalogue often fixes the depth for events that are thought to be shallow at 15 or 33 km, which are arbitrary but sensible values. The USGS CMT solutions use shorter time windows (typically body-wave data only) and higher frequencies than gCMT, which should give them a correspondingly better resolution of dip and and centroid depth. Use of even a few broad-band (*i.e.* unfiltered) records in the CMT inversion can increase the depth resolution considerably.

Although the CMT solutions are not constrained to be double-couple solutions (*i.e.* to result from slip on a fault), publications often use the 'best double-couple' versions of the solutions. In these versions the eigenvalue with the smallest absolute value is assigned to zero, while retaining the orientation of its eigenvector. The extent to which this 'best double-couple' solution is a good representation of the CMT solution can be assessed by the relative sizes of the original eigenvalues, one of which should have a much smaller absolute value than the other two, and ideally should be close to zero. For large earthquakes involving several sub-events of different orientations, large non-double couple components to the CMT solution are quite common. In general, the agreement between the strike, dip and rake of body-wave and 'best-double-couple' CMT solutions is usually quite good, though the rule is that if knowledge of the uncertainty really matters it is best to undertake sensitivity tests using body-wave analysis.

The seismologists' preferred measure of **earthquake size** is seismic moment (M_0), a scalar value defined as:

$$M_0 = \mu A \bar{u} \tag{9}$$

where μ is the rigidity (typically about 3×10^{10} Nm^{-2} in the crust), A is the fault rupture area and $\bar{u}$ is the average slip on the fault. M_0 is the absolute value of the two equal, but opposite, eigenvalues in the double-couple moment tensor and is therefore recoverable directly from the seismograms. Unlike the various definitions of earthquake magnitude, moment has a physical meaning that is easily understood, and is directly proportional to the amplitude of the seismogram at long periods. On the other hand its units are unfamiliar (Newton-metres), its values unwieldy (typically $\sim 10^{18}$ Nm for $\sim M_s$ 6.0), and there is a nostalgic and emotional attachment to the old magnitude scale and its more friendly range of values. For these reasons, people often use the 'moment-magnitude' (M_w), defined as

$$M_w = \frac{2}{3} \log_{10} M_0 - 6.0 \tag{10}$$

where M_o is in units of Nm. M_w and M_s are roughly comparable above moments of about 10^{19} Nm, but M_s saturates at high values, unlike M_w. For moments below $\sim 10^{19}$ Nm, M_w is larger than M_s as the slope of M_s *vs.* $\log M_0$ is close to 1 rather than 2/3.

In principle, the CMT methods should give a better estimate of M_0 than the body-wave methods because they use longer periods, which are a more stable indicator of moment. However, other factors contribute to uncertainties in the CMT moment. For both body-wave and CMT solutions there is often a trade-off between centroid depth, the duration of fault slip (called the 'time-function') and moment for small changes of depth in shallow earthquakes, particularly for dip-slip mechanisms (Fig. 5). This arises because the surface reflections often interfere destructively with the direct waves at shallow depths, requiring more moment to obtain the amplitude of the observed seismogram. Thus the uncertainty in the CMT depth can lead

to an uncertainty in the moment. Other factors can contribute to differences between CMT and body-wave estimates of moment, including different values of anelastic attenuation and different source velocity models. However, in most cases the CMT and body-wave moments agree to within about 10–20%, with the body-wave estimates often the lower of the two, as expected. A lot of effort is needed to prove any claim that a difference between the two is significant at this level.

With a sufficient appreciation of their limitations, the Harvard and USGS CMT catalogues are superb resources. If, however, you really care about the precise centroid depth or fault plane orientation, it is sensible to carry out higher-frequency body-wave modelling and the associated sensitivity tests. With a good distribution of stations, and SH as well as P waveforms, these body-wave techniques are capable of resolving centroid source parameters of simple earthquakes to within ±10º in strike and rake, ±5º in dip, ±3 km in depth as well as providing an estimate of moment.

The above discussion focuses on the use of teleseismic data to obtain average source parameters. Where sufficient data are available, particularly broad-band data from dense local networks, it is possible to extend these methods further to solve for greater detail, including both variations in the fault shape and variations in slip over fault surface [*e.g. Wald and Heaton*, 1994; *Wald et al.*, 1991].

Relationship between Strain and Seismic Moment Tensors

Kostrov [1974] showed that the strain of a volume, V, containing N earthquakes is related to the moment tensors of those earthquakes by:

$$\varepsilon_{ij} = \frac{1}{2\mu V} \sum_{n=1}^{N} M_{ij}^n \tag{11}$$

where ε_{ij} is the ijth component of the strain and $\mathbf{M}^n$ is the moment tensor of an earthquake contained in the volume. This relation assumes that there is no elastic strain stored within the volume; any such strain caused by one earthquake, must be released by other earthquakes, or relaxed aseismically. Strain, ε_{ij}, can be converted to strain rate $\dot{\varepsilon}_{ij}$ by dividing by the time interval of observation.
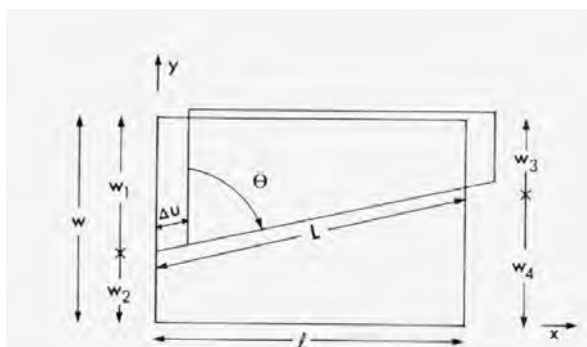
Figure 16: Map view of a rectangular region that is cut by a vertical fault of strike θ. The dimensions of the region are l, w, and thickness, h. *Note, however,* that this sketch could equally well apply to a cross-section of a region cut by a reverse fault or (if inverted) by a normal fault. The fault length, $L = l/\sin\theta$, and slip upon it, $\Delta u \ll l, w$.

Kostrov's paper is pretty impenetrable, and is not available electronically at the moment. The following derivation draws on *Molnar* [1983]. Consider a simple example, in which a single fault cuts across an entire region of width w in the $y-$direction, and length l in the $x-$direction (Figure 16); slip ΔU occurs on this fault. The Kostrov "trick" is to calculate the *average* strain that this slip causes throughout the volume. In the mathematics that follows, Δu can represent any of the following:

1. Slip in a single earthquake.

2. Total displacement on a fault over many earthquake 'cycles'.

3. Time-averaged slip rate on the fault.

In the first two of these cases, Kostrov's method yields an estimate of *Strain*, in the last case, Δu represents a rate of slip on the fault, and Kostrov's method yields *Strain Rate*.

The $yy-$component of strain (rate) is

$$\overline{\varepsilon}_{yy} = \frac{\Delta y}{w} = \frac{\Delta u \cos\theta}{w} \tag{12}$$

But the equivalent seismic moment (rate) to the slip (rate) is

$$M_0 = \mu L h \Delta u = \frac{\mu l h \Delta u}{\sin\theta} \tag{13}$$

here, μ is the shear modulus, and h is the thickness of the seismogenic layer.

Substituting into equation 12, we obtain

$$\bar{\varepsilon}_{yy} = M_0 \frac{\sin\theta\cos\theta}{\mu(lwh)} = M_0 \frac{\sin\theta\cos\theta}{\mu V} \tag{14}$$

where V is the volume of the region. The other two components of the strain are slightly more complicated to calculate. The mean displacement of the left and right sides of the body in Figure 16 are

$$\text{right} \quad \frac{\Delta u \sin\theta \; w_3}{w} \tag{15}$$
$$\text{left} \quad \frac{\Delta u \sin\theta \; w_1}{w},$$

so the *average* change in $x-$direction length of body is

$$\overline{\Delta l} = \frac{\Delta u \sin\theta(w_3 - w_1)}{w} \tag{16}$$

and, because $w_1 - w_3 = L\cos\theta$,

$$\bar{\varepsilon}_{xx} = \frac{\overline{\Delta l}}{l} = -\frac{\Delta u L \sin\theta\cos\theta}{wl} = -M_0 \frac{\sin\theta\cos\theta}{\mu V}. \tag{17}$$

Similarly, the mean $x-$displacement of the top and bottom sides of the region is

$$\frac{M_0 \sin^2\theta}{\mu V}, \tag{18}$$

and the mean $y-$displacement of the right and left sides is

$$-\frac{M_0 \cos^2\theta}{\mu V}, \tag{19}$$

so

$$\bar{\varepsilon}_{xy} = \frac{1}{2}\frac{M_0}{\mu V}\left(\sin^2\theta - \cos^2\theta\right) \tag{20}$$

Recall the definition of the moment tensor

$$M_{ij} = M_0(\hat{u}_i\hat{n}_j + \hat{u}_j\hat{n}_i) \tag{21}$$

where $\hat{\mathbf{u}}$ and $\hat{\mathbf{n}}$ are unit vectors in the directions parallel to the slip and perpendicular to the fault plane,

$$\hat{\mathbf{u}} = (\sin\theta, \cos\theta, 0) \tag{22}$$
$$\hat{\mathbf{n}} = (-\cos\theta, \sin\theta, 0).$$

We can see that the increment of strain associated with the slip on this fault is

$$\bar{\varepsilon}_{ij} = \frac{M_{ij}}{2\mu V}. \tag{23}$$

Illustration of Kostrov's relation using a simple example

The total moment released in earthquakes in California since the 1906, M_w 7.9, San Francisco earthquake has been 8×10^{20} N m. Is the rate of moment release consistent with the relative plate motion across the region?

Treat the zone of active deformation in California as a rectangle, 1000 km long in the NW-SE direction, and 400 km wide. You may assume that all earthquakes in the region occur by right-lateral strike slip on vertical planes striking 135°. The relative motion of the Pacific plate with respect to the North American plate in this region is 35 mm/yr in the direction 315°.

Rotate coordinates so that one axis is along strike. Here, I choose x. $\hat{n}$ is the unit vector perpendicular to the fault plane, $\hat{u}$ is the unit vector describing the slip of the block towards which $\hat{n}$ is pointing (for all faults except vertical ones, this is more usually called the hanging wall).

$$\hat{n} = (0,1,0) \qquad M_{ij} = u_i n_j + u_j n_i$$

$$\hat{u} = (-1,0,0) \qquad \mathbf{M} = \begin{bmatrix} 0 & -1 & 0 \\ -1 & 0 & 0 \\ 0 & 0 & 0 \end{bmatrix}$$
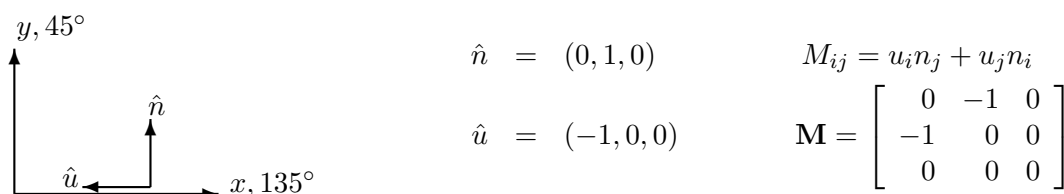
$$\dot{\varepsilon}_{ij} = \frac{M_{ij}}{2\mu lwst} \qquad \text{(Kostrov)}$$

$$\dot{\varepsilon}_{12} = \frac{M_{12}}{2\mu lwst}$$

or

$$\Delta v = w \times \frac{\partial u_x}{\partial y} = w \times 2\dot{\varepsilon}_{12} = \frac{M_{12}}{\mu lst}$$

where Δv is velocity difference, l is length of zone, w is width, s is seismogenic thickness, and t is time interval. All 30 points were given if the candidate went straight to the expression for strain rate or velocity difference, provided it was clear that they knew what they were doing.

About half of the velocity difference is expressed seismically:

$$\Delta v \sim \frac{8 \times 10^{20}\text{N m}}{3 \times 10^{10}\text{N m}^{-2} \times 10^6\text{m} \times 15 \times 10^3\text{m} \times 110\text{years}} \quad \sim \quad 18 \text{ mm/yr}$$

Here, I have assumed $s = 15$ km.

The missing moment release is approximately equivalent to the moment of the 1906 earthquake:

$$M_0 = 10^{1.5\times(7.9+6.0)} \sim 7 \times 10^{20}\text{N m}$$

Bibliography

Berberian, M., J. A. Jackson, M. Qorashi, M. M. Khatib, K. Priestley, M. Talebian, and M. Ghafuri-Ashtiani, The 1997 May 10 Zirkuh (Qa'enat) earthquake (M_W 7.2): faulting along the Sistan suture zone of eastern Iran, *Geophys. J. Int.*, *136*(3), 671–694, 1999.

Calais, E., L. Dong, M. Wang, Z. Shen, and M. Vergnolle, Continental deformation in Asia from a combined GPS solution, *Geophysical Research Letters*, *33*(24), L24,319, doi: 10.1029/2006GL028433, 2006.

Cowie, P., and C. Scholz, Displacement-length scaling relationship for faults: data synthesis and discussion, *J Struct Geol*, *14*(10), 1149–1156, 1992.

De Mets, C., R. G. Gordon, D. F. Argus, and S. Stein, Current plate motions, *Geophys. J. Int.*, *101*, 425–478, 1990.

Dziewonski, A. M., T.-A. Chou, and J. H. Woodhouse, Determination of earthquake source parameters from waveform data for studies of global and regional seismicity, *J. Geophys. Res.*, *86*(B4), 2825–2852, 1981.

Ekström, G., M. Nettles, and A. Dziewonski, The Global CMT Project 2004–2010: centroid-moment tensors for 13,017 earthquakes, *Phys. Earth Planet Inter.*, *200-201*, 1–9, 2012.

Engdahl, E. R., R. van der Hilst, and R. Buland, Global teleseismic earthquake relocation with improved travel times and procedures for depth determination, *Bull. Seismol. Soc. Amer.*, *88*(3), 722–743, 1998.

Gan, W., P. Zhang, Z.-K. Shen, Z. Niu, M. Wang, Y. Wan, D. Zhou, and J. Cheng, Present-day crustal motion within the Tibetan plateau inferred from GPS measurements, *J. Geophys. Res.*, *112*(B8), 14, 2007.

Haessler, H., A. Deschamps, H. Dufumier, H. Fuenzalida, and A. Cisternas, The rupture process of the Armenian earthquake from broad-band teleseismic records, *Geophys. J. Int.*, *109*, 151–161, 1992.

http://www.globalcmt.org, Global CMT project.

Isacks, B., J. Oliver, and L. Sykes, Seismology and the new global tectonics, *J. Geophys. Res.*, *73*, 5855–5899, 1968.

Kostrov, B., Seismic moment and energy of earthquakes, and seismic flow of rock, *Izv. Acad. Sci. USSR Phys. Solid Earth*, *97*, 23–44, 1974.

Bibliography

McCaffrey, R., and J. Nábĕlek, Earthquakes, gravity and the origin of the Bali Basin: an example of a nascent continental fold-and-thrust belt, *J. Geophys. Res.*, *92*(B1), 441–460, 1987.

McKenzie, D., and R. Parker, The North Pacific: An example of tectonics on a sphere, *Nature*, *216*, 1276–1280, 1967.

Molnar, P., Average regional strain due to slip on numerous faults of different orientations, *J. Geophys. Res.*, *88*(B8), 6,430–6,432, 1983.

Molnar, P., and P. Tapponnier, Cenozoic tectonics of Asia: effects of a continental collision, *Science*, *189*, 419–426, 1975.

Morgan, W., Rises, trenches, great faults, and crustal blocks, *J. Geophys. Res.*, *73*, 1959–1982, 1968.

Nocquet, J.-M., Present-day kinematics of the Mediterranean: A comprehensive overview of GPS results, *Tectonophysics*, pp. 1–23, doi:10.1016/j.tecto.2012.03.037, 2012.

Shearer, P. M., *Introduction to seismology*, Cambridge University PressUniversity Press, 1999.

Stein, S., and J. Stein, Shallow versus deep uncertainties in natural hazard assessments, *Eos*, 2013.

Tapponnier, P., and P. Molnar, Slip-line field theory and large-scale continental tectonics, *Nature*, *264*, 319, 1976.

Wald, D., and T. Heaton, Spatial and temporal distribution of slip for the 1992 Landers, California, earthquake, *Bull. Seismol. Soc. Amer.*, *84*, 668–691, 1994.

Wald, D., D. Helmberger, and T. Heaton, Rupture model of the 1989 Loma Prieta earthquake from the inversion of strong-motion and broadband teleseismic data, *Bull. Seis. Soc. Am.*, *81*, 1540–1572, 1991.

Wallace, L. M., J. Beavan, R. McCaffrey, K. Berryman, and P. Denys, Balancing the plate motion budget in the South Island, New Zealand using GPS, geological and seismological data, *Geophys J Int*, *168*(1), 332–352, 2007.

Zubovich, A. V., et al., GPS velocity field for the Tien Shan and surrounding regions, *Tectonics*, *29*(6), TC6014, doi:10.1029/2010TC002772, 2010.